Instability In Magnetic Nozzle and Spectral Pollution

Hunt Feng

May 31, 2023

Contents

Abstract

Spectral theory is a common technique for analyzing the instability of a dynamical system. By discretizing the linearized equations motion of magnetic nozzle, the instability problem becomes an algebraic eigenvalue problem. Given Dirichlet boundary condition, we found that the flow in magnetic nozzle is stable. Different discretizations, such as finite difference, finite element and spectral element method agree with each other. By studying the convergence of different modes, we successfully eliminated the spurious unstable modes occur in supersonic and transonic cases.

Chapter 1

Introduction

[1]

1.1 Plasma

In this thesis we study the instability of plasma flow in magnetic mirror configuration. We start the thesis by introducing the concept of plasma.

Plasma is one of the four fundamental states of matter, along with solids, liquids, and gases. It is often referred to as the fourth state of matter. Plasma is an ionized gas that consists of highly energized particles, including positively charged ions and negatively charged electrons.

[[Put a figure made by professor Andrei!!!!!!!!!!!!!!!!!]]

In a plasma, the atoms or molecules have been stripped of their electrons, resulting in a collection of charged particles. This ionization process occurs when a gas is subjected to extremely high temperatures or strong electromagnetic fields, which supply sufficient energy to overcome the electrostatic forces that hold electrons in their orbits around atomic nuclei.

Plasma is known for its unique properties. It is an excellent conductor of electricity and is strongly influenced by electromagnetic fields. Plasma also emits light, and examples of natural plasma include stars, such as our Sun, and lightning. Artificially generated plasma can be found in fluorescent lights, plasma televisions, and certain types of industrial torches.

In addition to these applications, plasma has various scientific and technological uses. It is used in plasma physics research, nuclear fusion experiments, plasma cutting and welding, plasma medicine for treating diseases, and even in spacecraft propulsion systems.

Overall, plasma is an intriguing and versatile state of matter with significant implications in various fields of science, technology, and industry.

1.2 Magnetic Mirror Configuration

In this thesis, we are going to deal with plasma flow in magnetic mirror configuration. The magnetic mirror configuration is a concept in plasma physics and magnetic confinement fusion research. It involves using magnetic fields to confine and control the movement of charged particles, typically in a linear or cylindrical geometry.

In a magnetic mirror configuration, a combination of magnetic field lines is employed to create regions of high magnetic field strength called "magnetic mirrors" or "mirror cells." These magnetic mirrors can trap and reflect charged particles, such as ions or electrons, preventing them from escaping along the magnetic field lines. The particles are confined within the magnetic mirrors, bouncing back and forth between the mirror cells.

The concept of a magnetic mirror has connections to both the magnetic nozzle and solar wind:

1. Magnetic Nozzle: A magnetic nozzle is a device that uses a magnetic field to shape and control the flow of charged particles in a plasma propulsion system. By employing magnetic mirrors, the magnetic nozzle can efficiently direct and accelerate the plasma particles, generating thrust for propulsion. The magnetic field in the nozzle helps collimate and focus the plasma exhaust, increasing its velocity and enhancing the performance of the propulsion system.

2. Solar Wind: The solar wind is a stream of charged particles, primarily electrons and protons, flowing outward from the Sun. The interaction between the solar wind and the Earth's magnetic field is of particular importance. The Earth's magnetic field acts as a barrier, deflecting and trapping the charged particles from the solar wind. This trapping effect is similar to the magnetic mirror configuration, where the Earth's magnetic field lines create mirror cells that confine and redirect the solar wind particles, forming the Van Allen radiation belts.

In summary, the magnetic mirror configuration is a technique that uses magnetic fields to confine and control charged particles. It finds applications in plasma propulsion systems through the use of a magnetic nozzle. Moreover, the concept of magnetic mirrors is relevant to the study of the interaction between the solar wind and the Earth's magnetic field, as it helps in understanding the trapping and confinement of charged particles in the Van Allen radiation belts.

1.3 Instability of Plasma Flow

Since we are going to study the instability of the plasma flow in magnetic mirror configuration. We need to understand the concept of plasma instability. The instability of plasma flow refers to the tendency of a plasma system to deviate from a stable, equilibrium state and exhibit perturbations or fluctuations in its behavior. These instabilities can arise from various factors, such as the interaction of particles with electromagnetic fields, collective effects, or the presence of gradients in plasma parameters.

Understanding and studying plasma instabilities are crucial for several reasons:

1. Energy Transport: Plasma instabilities can play a significant role in the transport of energy within a plasma system. They can enhance or hinder the transfer of energy between particles, affecting the overall efficiency and behavior of plasma devices. By studying these instabilities, scientists and engineers can gain insights into the mechanisms governing energy transport in plasmas and develop strategies to control and mitigate them.

2. Plasma Confinement: In applications such as magnetic confinement fusion, achieving and maintaining a high degree of plasma confinement is essential for sustained fusion reactions. Instabilities can lead to the loss of plasma particles, reduction in confinement time, and decreased overall plasma performance. By understanding the nature of these instabilities, researchers can design improved confinement strategies and develop techniques to suppress or stabilize them.

3. Plasma Heating: Instabilities can also influence the heating mechanisms in a plasma system. For example, in magnetic fusion devices, instabilities like the ion temperature gradient (ITG) or electron temperature gradient (ETG) instabilities can hinder efficient heating of the plasma. Understanding these instabilities helps in optimizing heating schemes and improving the overall heating efficiency of plasmas.

4. Plasma Diagnostics: Instabilities can manifest as measurable fluctuations in plasma parameters such as density, temperature, and electromagnetic fields. By studying these fluctuations and their characteristics, scientists can employ diagnostic techniques to gain valuable information about the plasma state, identify the presence of instabilities, and assess the stability and health of plasma devices.

Overall, the study of plasma instabilities is crucial for advancing plasma physics research, optimizing plasma devices, and improving our ability to control and utilize plasmas effectively in various applications such as fusion energy, plasma propulsion, materials processing, and astrophysics.

1.4 Goals of this Thesis

The major goal of this thesis is to study the instability of plasma flow in magnetic mirror configuration with different boundary conditions.

Fluid model of plasma will be reviewed and linearized governing equations will be derived in chapter 2. The problem will be then formulated as an eigenvalue problem.

In chapter 3, spectral method and shooting method for solving eigenvalue problem will be introduced. In the section of spectral method, different discretizations of the operators, such as finite difference and spectral method will be discussed. Moreover, spectral pollution and its filtering will as also be investigated.

Then in the next section, we will formulate the problem to the form suitable

for applying shooting method. We will apply both shooting method and spectral method to the problem. By comparing the results from two different methods, the credibility of the results are increased.

In chapter 4, we ill use the method developed in chapter 3 to conduct numerical experiments. The goal is to extract the eigenvalues (frequency) of each oscillating mode.

Conclusion will in chapter 5.

Chapter 2

Governing Equations

2.1 Single Particle Motion Along Magnetic Field Line

The motion of charged particles in magnetic field is determined by the magnetic force,

$$m\frac{\mathrm{d}\mathbf{v}}{\mathrm{d}t} = q\mathbf{v}\times\mathbf{B}$$

where m is the mass of charged particle, and q is the charge of particles.

Consider a magnetic field pointing in z-direction, $\mathbf{B} = B\hat{\mathbf{z}}$. Since the magnetic force is perpendicular to both $\mathbf{v}$ and $\mathbf{B}$, we can separate the equation of motion into two directions,

$$q\mathbf{v}_\perp\times\mathbf{B} = \frac{mv_\perp^2}{r}\hat{\mathbf{r}}, \quad \mathbf{v}_\parallel = v_\parallel\hat{\mathbf{z}}$$

where $\mathbf{v}_\perp$ is the velocity perpendicular to the magnetic field, and $\mathbf{v}_\parallel$ is the velocity parallel to the magnetic field. In this way, we see that the charged particle gyrates about the magnetic field, doing helical motion along the magnetic field line.

Moreover, if we assume a static, nonuniform $\mathbf{B}$ field, the particles will stay on the same magnetic field line due to the so-called longitudinal invariant

$$J = \int_a^b v_\parallel ds$$

where $[a, b]$ is the region of magnetic nozzle.

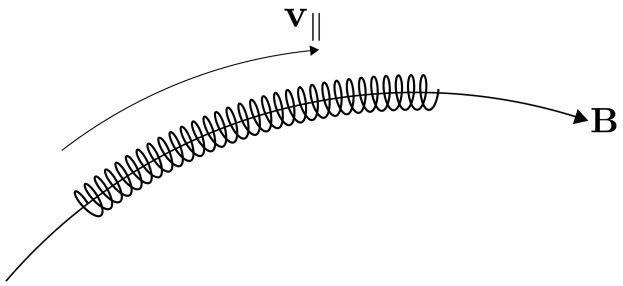

Figure 2.1: A charged particle gyrates about the magnetic field line. The velocity along the field line is $\mathbf{v}_{\parallel}$ and the gyrate frequency, radius is given by the radial equation, $q\mathbf{v}_{\perp} \times \mathbf{B} = \hat{\mathbf{r}} m v_{\perp}^2 / r$. Moreover, for static, nonuniform magnetic field, the charged particle will stay on the same of magnetic field line as it gyrates.

2.2 From Kinetic Theory to Fluid Description

In kinetic theory, the charged particles in plasma obey a certain distribution function $f(\mathbf{x}, \mathbf{v}, t)$. This distribution function is affected by plasma temperature. Assuming there is only one species of particles in the plasma, the plasma temperature is just the sum of the kinetic energy of all particles. We expect at higher temperature, faster the particles will be.

At equilibrium, the particles can be characterized by Maxwell-Boltzmann distribution

$$f_M(\mathbf{x}, \mathbf{v}, t) = \frac{1}{(\pi v_{th}^2)^{3/2}} \exp\left(- \left(\frac{v}{v_{th}} \right)^2 \right)$$

where $v_{th} = \sqrt{2k_B T/m}$ is the thermal velocity.

The moments of the distribution function are suitable macroscopic properties of the plasma. For example, the plasma density and plasma momentum can be viewed as

$$n(\mathbf{x}, t) = \int_{\mathbb{R}^3} f(\mathbf{x}, \mathbf{v}, t) d^3\mathbf{v}$$

$$n\mathbf{V}(\mathbf{x}, t) = \int_{\mathbb{R}^3} \mathbf{v} f(\mathbf{x}, \mathbf{v}, t) d^3\mathbf{v}$$

where $\mathbf{V}$ is the fluid velocity of the charged particle. It is the bulk velocity of the plasma. In magnetic nozzle, since the charged particles flow along the magnetic field line, it is intuitive to think of $\mathbf{V}$ as the plasma flow velocity along the magnetic field line.

In fusion device and space propulsion system, we want high plasma temperature to achieve good performance. Hence, we assume high plasma temperature in this thesis. In other words, the plasma is collisionless.

The distribution function f in a collisionless plasma satisfies the so-called collisionless Vlasov equation, $\mathrm{d}/\mathrm{d}t\ f(\mathbf{x},\mathbf{v},t)=0$. Expand it explicitly, it is

$$\frac{\partial f}{\partial t}+\mathbf{v}\frac{\partial f}{\partial \mathbf{x}}+\frac{q}{m}(\mathbf{E}+\mathbf{v}\times\mathbf{B})\frac{\partial f}{\partial \mathbf{v}}=0 \tag{2.1}$$

where $q(\mathbf{E}+\mathbf{v}\times\mathbf{B})$ is the Lorentz force experience by the species, the collision term $C(f)$ is dropped. Worth to mention that the electric field and magnetic field are generated by the configuration and the motion of the charged particles.

Integrate both sides with respect to volume element in velocity space, $d^3\mathbf{v}$, we get the conservation of density.

$$\frac{\partial \rho}{\partial t}+\boldsymbol{\nabla}\cdot(\rho\mathbf{V})=0$$

If we multiply $\mathbf{v}$ on both sides and integrate with respect to $d^3\mathbf{v}$, we get the conservation of momentum.

$$\rho\frac{\partial \mathbf{V}}{\partial t}+\mathbf{V}\cdot\boldsymbol{\nabla}\mathbf{V}=\frac{q}{m}(\mathbf{E}+\mathbf{V}\times\mathbf{B})-\boldsymbol{\nabla}p$$

In the process we assume isotropic pressure, and no viscosity exists in the plasma.

As we can see the fluid description only depends on the macroscopic properties of plasma, such as the fluid velocity along the magnetic field line $\mathbf{V}$, density ρ, and pressure p of the plasma. This simplifies the problem.

2.3 Governing Equations for Flow in Magnetic Nozzle

In this section, we will derive the governing equations of the flow in magnetic nozzle, starting from the fluid description for plasma.

In magnetic nozzle, the magnetic field is along the nozzle, which we denote as z-axis. Due to Lorentz force, the charged particles gyrates about the magnetic field lines. Because the magnetic moment is invariant in such situation (**reference**). The fluid velocity of particles can be written as $\mathbf{v}=v\mathbf{B}/B$, meaning that the particles move along the magnetic field lines. Therefore the conservation of density

$$\frac{\partial n}{\partial t}+\boldsymbol{\nabla}\cdot(n\mathbf{v})=0\Rightarrow\frac{\partial n}{\partial t}+B\frac{\partial}{\partial z}\Big(\frac{nv}{B}\Big)=0$$

In the derivation, $\boldsymbol{\nabla}\cdot\mathbf{B}=0$ is used.

To derive the second governing equation, we start from the conservation of momentum,

$$\frac{\partial v}{\partial t}+v\frac{\partial v}{\partial z}=-\frac{1}{\rho}\boldsymbol{\nabla}p$$

Let $\boldsymbol{\nabla} p = k_B T \, \partial n/\partial z$, we have

$$\frac{\partial v}{\partial t} + v\frac{\partial v}{\partial z} = -c_s^2 \frac{1}{n}\frac{\partial n}{\partial z}$$

where $c_s^2 = k_B T/m$ is the square of sound speed.

Therefore the dynamics of the flow in magnetic nozzle can be characterized by the conservation of density and momentum,

$$\frac{\partial n}{\partial t} + B\frac{\partial}{\partial z}\left(\frac{nv}{B}\right) = 0$$
$$\frac{\partial v}{\partial t} + v\frac{\partial v}{\partial z} = -c_s^2 \frac{1}{n}\frac{\partial n}{\partial z}$$

The discussion of magnetic field is in next subsection.

2.3.1 Magnetic Field in Magnetic Nozzle

In 1D problem, the magnetic field is given by

$$B(z) = B_0 \left[1 + R\exp\left(-\left(\frac{x}{\delta}\right)^2\right)\right]$$

where $1 + R$ is the magnetic mirror ratio, and δ determines the spread of the magnetic field. It is shown in Fig.(2.2).

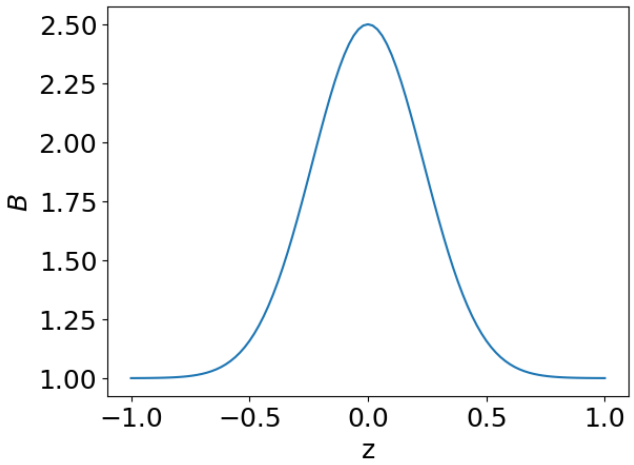

Figure 2.2: This is the magnetic field in nozzle with mirror ratio $1 + R = B_{max}/B_{min} = 2.5$, and the spread of magnetic field, $\delta = 0.1/0.3 = 0.\bar{3}$.

2.3.2 Velocity Profile at Equilibrium

Let n_0 and v_0 be the density and velocity at equilibrium (stationary solution), we know that $\partial n_0/\partial t = 0$ and $\partial v_0/\partial t = 0$, therefore n_0 and v_0 satisfy the

so-called equilibrium condition,

$$\frac{\partial}{\partial z}\Big(\frac{n_0 v_0}{B}\Big) = 0$$
$$v_0 \frac{\partial v_0}{\partial z} = -c_s^2 \frac{1}{n_0}\frac{\partial n_0}{\partial z}$$

Let $M(z) = v_0(z)/c_s$ be the mach number (nondimensionalized velocity). The equations of motion become

$$B\frac{\partial}{\partial z}\left(\frac{n_0 M}{B}\right) = 0$$
$$M\frac{\partial M}{\partial z} = -\frac{1}{n_0}\frac{\partial n_0}{\partial z}$$

Substitute $\frac{1}{n_0}\,\partial n_0/\partial z$ using first equation, the conservation of momentum becomes

$$(M^2 - 1)\frac{\partial M}{\partial z} = -\frac{M}{B}\frac{\partial B}{\partial z}$$

Notice that there is a singularity at $M = 1$, the sonic speed.

This is a separable equation, integrate it and use the conditions at midpoint $B(0) = B_m, M(0) = M_m$ we get

$$M^2 e^{-M^2} = \frac{B^2}{B_m^2} M_m^2 e^{-M_m^2}$$

We can now express M using the Lambert W function,

$$M(z) = \left[-W_k\left(-\frac{B(z)^2}{B_m^2} M_m^2 e^{-M_m^2}\right)\right]^{1/2}$$

where the subscript k of W stands for branch of Lambert W function. When $k = 0$, it is the subsonic branch; When $k = -1$, it is the supersonic branch. Below shows a few cases of the solution.

- $M_m < 1, k = 0$, subsonic velocity profile.
- $M_m = 1$, $k = 0$ for $x < 0$ and $k = -1$ for $x > 0$, accelerating profile
- $M_m = 1$, $k = -1$ for $x < 0$ and $k = 0$ for $x > 0$, decelerating profile
- $M_m > 1, k = -1$, supersonic velocity profile

Fig.(2.3) shows some cases of the solution.

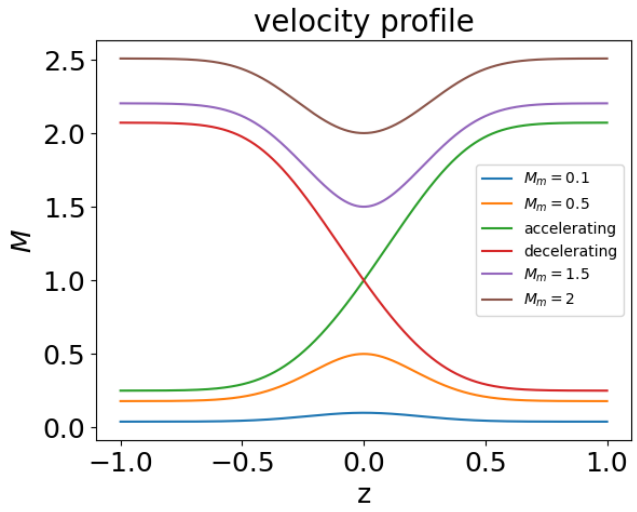

Figure 2.3: The velocity profile in the magnetic nozzle is completely determined by M_m, the velocity at the midpoint, $z = 0$. For the transonic velocity profiles, M_m alone is not enough to determine the profile, we need to specify the branch of Lambert W function to determine whether it is accelerating or decelerating.

2.4 Linearized Equations

For convenience, we nondimensionalize the governing equations by normalizing the velocity to c_s, $v \mapsto v/c_s$, z to system length L, $z \mapsto z/L$ and time $t \mapsto c_s t/L$. The governing equations become

$$\frac{\partial n}{\partial t} + n\frac{\partial v}{\partial z} + v\frac{\partial n}{\partial z} - nv\frac{\partial_z B}{B} = 0 \tag{2.2}$$

$$n\frac{\partial v}{\partial t} + nv\frac{\partial v}{\partial z} = -\frac{\partial n}{\partial z} \tag{2.3}$$

and the nondimensionalized equilibrium condition is

$$\frac{\partial}{\partial z}\left(\frac{n_0 v_0}{B}\right) = 0 \tag{2.4}$$

$$v_0\frac{\partial v_0}{\partial z} = -\frac{1}{n_0}\frac{\partial n_0}{\partial z} \tag{2.5}$$

Now we are going to derive an important intermediate result, the linearized governing equations.

Proposition 1. *Let $n = n_0(z) + \tilde{n}(z,t)$ and $v = v_0(z) + \tilde{v}(z,t)$, where $\tilde{n}$ and $\tilde{v}$*

are small perturbed quantities. The linearized governing equations are

$$\frac{1}{n_0}\frac{\partial \tilde{n}}{\partial t} + \frac{\partial \tilde{v}}{\partial z} + v_0\tilde{Y} + \tilde{v}\frac{\partial_z n_0}{n_0} - \tilde{v}\frac{\partial_z B}{B} = 0 \tag{2.6}$$

$$\frac{\partial \tilde{v}}{\partial t} + \frac{\partial (v_0\tilde{v})}{\partial z} = -\tilde{Y} \tag{2.7}$$

where

$$\tilde{Y} \equiv \frac{1}{n_0}\frac{\partial \tilde{n}}{\partial z} - \frac{\partial_z n_0}{n_0^2}\tilde{n} = \frac{\partial}{\partial z}\left(\frac{\tilde{n}}{n_0}\right)$$

Proof. We first derive Eq.(2.6). We linearize Eq.(2.4) by setting $n = n_0 + \tilde{n}$ and $v = v_0 + \tilde{v}$. By ignoring the second order perturbations, we obtain

$$\begin{aligned}
&\frac{\partial (n_0+\tilde{n})}{\partial t} + (n_0+\tilde{n})\frac{\partial (v_0+\tilde{v})}{\partial z} + (v_0+\tilde{v})\frac{\partial (n_0+\tilde{n})}{\partial z} - (n_0+\tilde{n})(v_0+\tilde{v})\frac{\partial_z B}{B} = 0 \\
\Rightarrow &\frac{\partial \tilde{n}}{\partial t} + n_0\frac{\partial v_0}{\partial z} + \tilde{n}\frac{\partial v_0}{\partial z} + n_0\frac{\partial \tilde{v}}{\partial z} + v_0\frac{\partial n_0}{\partial z} + \tilde{v}\frac{\partial n_0}{\partial z} + v_0\frac{\partial \tilde{n}}{\partial z} - (n_0 v_0 + n_0\tilde{v} + \tilde{n}v_0)\frac{\partial_z B}{B} = 0 \\
\Rightarrow &\frac{1}{n_0}\frac{\partial \tilde{n}}{\partial t} + \frac{\partial v_0}{\partial z} + \frac{\tilde{n}}{n_0}\frac{\partial v_0}{\partial z} + \frac{\partial \tilde{v}}{\partial z} + \frac{v_0}{n_0}\frac{\partial n_0}{\partial z} + \frac{\tilde{v}}{n_0}\frac{\partial n_0}{\partial z} + \frac{v_0}{n_0}\frac{\partial \tilde{n}}{\partial z} - v_0\frac{\partial_z B}{B} - \tilde{v}\frac{\partial_z B}{B} - \tilde{n}\frac{v_0}{n_0}\frac{\partial_z B}{B} = 0
\end{aligned}$$

Using the equilibrium condition Eq.(2.4), some of the terms are canceled and the last term can be written as

$$\tilde{n}\frac{v_0}{n_0}\frac{\partial_z B}{B} = \frac{\tilde{n}}{n_0}\left(\frac{\partial_z n_0}{n_0}v_0 + \frac{\partial v_0}{\partial z}\right)$$

Now, we are left with equation

$$\frac{1}{n_0}\frac{\partial \tilde{n}}{\partial t} + \frac{\partial \tilde{v}}{\partial z} + v_0\underbrace{\left(\frac{1}{n_0}\frac{\partial \tilde{n}}{\partial z} - \frac{\tilde{n}}{n_0}\frac{\partial_z n_0}{n_0}\right)}_{\tilde{Y}} + \frac{\tilde{v}}{n_0}\frac{\partial n_0}{\partial z} - \tilde{v}\frac{\partial_z B}{B} = 0$$

To derive Eq.(2.7), we linearize the LHS of the conservation of momemtum

$$\begin{aligned}
&(n_0+\tilde{n})\frac{\partial (v_0+\tilde{v})}{\partial t} + (n_0+\tilde{n})(v_0+\tilde{v})\frac{\partial (v_0+\tilde{v})}{\partial z} = -\frac{\partial n}{\partial z} \\
\Rightarrow &\frac{\partial v_0}{\partial t} + \frac{\tilde{n}}{n_0}\frac{\partial v_0}{\partial t} + \frac{\partial \tilde{v}}{\partial t} + \left(v_0 + \tilde{v} + \frac{\tilde{n}}{n_0}v_0\right)\frac{\partial (v_0+\tilde{v})}{\partial z} = -\frac{1}{n_0}\frac{\partial n}{\partial z} \\
\Rightarrow &\frac{\partial v_0}{\partial t} + v_0\frac{\partial v_0}{\partial z} + \tilde{v}\frac{\partial v_0}{\partial z} = -\frac{1}{n_0}\frac{\partial n_0}{\partial z} - \frac{1}{n_0}\frac{\partial \tilde{n}}{\partial z} - v_0\frac{v_0}{z} - \frac{\tilde{n}}{n_0}v_0\frac{\partial v_0}{\partial z}
\end{aligned}$$

Using the equilibrium condition Eq.(2.5) on the RHS, we get the desired form. □

2.5 Formulation of the Problem

In order to investigate the instability of magnetic nozzle, we need formulate it as an eigenvalue problem. To do that, we assume the perturbed density and velocity are oscillatory, i.e. $\tilde{n}, \tilde{v} \sim \exp(-i\omega t)$, where ω is the oscillation frequency of the perturbed quantities. This frequency can be a complex number. If $\omega = \omega_r + i\omega_i$, then the perturbed quantities becomes $\tilde{n} \sim \exp(\omega_i t)\exp(i\omega_r t)$, which means it grows exponentially with time.

The first step, we can combine Eq.(2.6) and Eq.(2.7) into 1 equation.

Proposition 2.

$$\frac{\partial}{\partial z}\ln\Big(\frac{n_0}{B}\Big) = -\frac{1}{v_0}\frac{\partial v_0}{\partial z} \tag{2.8}$$

Proof.

$$\frac{\partial}{\partial z}\ln\Big(\frac{n_0}{B}\Big) = \frac{B}{n_0}\frac{\partial}{\partial z}\Big(\frac{n_0}{B}\Big) = \frac{1}{n_0}\frac{n_0}{z} + B\frac{\partial}{\partial z}\left(\frac{1}{B}\right) = \frac{1}{n_0}\frac{n_0}{z}\underbrace{-\frac{1}{n_0 v_0}\frac{\partial n_0 v_0}{\partial z}}_{Eq.(2.4)} = -\frac{1}{v_0}\frac{\partial v_0}{\partial z}$$

□

Proposition 3. *Let $\tilde{n} \sim \exp(-i\omega t)$ and $\tilde{v} \sim \exp(-i\omega t)$, then we have the polynomial eigenvalue problem*

$$\omega^2\tilde{v} + 2i\omega\left(v_0\frac{\partial}{\partial z} + \frac{\partial v_0}{\partial z}\right)\tilde{v} + \left[(1-v_0^2)\frac{\partial^2}{\partial z^2} - \left(3v_0 + \frac{1}{v_0}\right)\frac{\partial v_0}{\partial z}\frac{\partial}{\partial z} - \left(1 - \frac{1}{v_0^2}\right)\left(\frac{\partial v_0}{\partial z}\right)^2 - \left(v_0 + \frac{1}{v_0}\right)\frac{\partial^2 v_0}{\partial z^2}\right]\tilde{v} = 0 \tag{2.9}$$

Proof.

$$\begin{aligned}
&\frac{1}{n_0}\frac{\partial \tilde{n}}{\partial t} + \frac{\partial \tilde{v}}{\partial z} + v_0\tilde{Y} + \tilde{v}\frac{\partial_z n_0}{n_0} - \tilde{v}\frac{\partial_z B}{B} = 0\\
&\frac{\partial \tilde{v}}{\partial t} + \frac{\partial(v_0\tilde{v})}{\partial z} = -\tilde{Y}
\end{aligned}$$

We plug Eq.(2.7) in to Eq.(2.6), we have

$$-i\omega\frac{\tilde{n}}{n_0} + \frac{\partial \tilde{v}}{\partial z} - v_0\left(-i\omega\tilde{v} + \frac{\partial(v_0\tilde{v})}{\partial z}\right) + \tilde{v}\frac{\partial_z n_0}{n_0} - \tilde{v}\frac{\partial_z B}{B} = 0$$

Using the equilibrium condition Eq.(2.4), we can eliminate the term $\partial_z B/B$,

$$\begin{aligned}
&-i\omega\frac{\tilde{n}}{n_0} + \frac{\partial \tilde{v}}{\partial z} + v_0\left(i\omega\tilde{v} - v_0\frac{\partial \tilde{v}}{\partial z} - \tilde{v}\frac{\partial v_0}{\partial z}\right) - \tilde{v}\frac{\partial_z v_0}{v_0} = 0\\
\Rightarrow &-i\omega\frac{\tilde{n}}{n_0} + i\omega v_0\tilde{v} + (1-v_0^2)\frac{\partial \tilde{v}}{\partial z} - \left(v_0 + \frac{1}{v_0}\right)\frac{\partial v_0}{\partial z}\tilde{v} = 0
\end{aligned}$$

Now we take $\partial/\partial t$ on Eq.(2.7). Recall the fact that $\tilde{Y} = \partial(\tilde{n}/n_0)/\partial z$, we have

$$\omega^2\tilde{v} + i\omega\left(v_0\frac{\partial\tilde{v}}{\partial z} + \tilde{v}\frac{\partial v_0}{\partial z}\right) = \frac{\partial}{\partial t}\frac{\partial}{\partial z}\left(\frac{\tilde{n}}{n_0}\right)$$

$$\Rightarrow \omega^2\tilde{v} + i\omega\left(v_0\frac{\partial\tilde{v}}{\partial z} + \tilde{v}\frac{\partial v_0}{\partial z}\right) = \frac{\partial}{\partial z}\left(-i\omega v_0\tilde{v} - (1-v_0^2)\frac{\partial\tilde{v}}{\partial z} + \left(v_0 + \frac{1}{v_0}\right)\frac{\partial v_0}{\partial z}\tilde{v}\right)$$

Expand the RHS and collect terms, we get

$$\omega^2\tilde{v}$$
$$+ 2i\omega\left(v_0\frac{\partial}{\partial z} + \frac{\partial v_0}{\partial z}\right)\tilde{v}$$
$$+ \left[(1-v_0^2)\frac{\partial^2}{\partial z^2} - \left(3v_0 + \frac{1}{v_0}\right)\frac{\partial v_0}{\partial z}\frac{\partial}{\partial z} - \left(1 - \frac{1}{v_0^2}\right)\left(\frac{\partial v_0}{\partial z}\right)^2 - \left(v_0 + \frac{1}{v_0}\right)\frac{\partial^2 v_0}{\partial z^2}\right]\tilde{v} = 0$$

□

Next step we can decouple this equation so that it becomes an eigenvalue problem.

$$\begin{bmatrix} 0 & 1 \\ \hat{M} & \hat{N} \end{bmatrix}\begin{bmatrix} \tilde{v} \\ \omega\tilde{v} \end{bmatrix} = \omega\begin{bmatrix} \tilde{v} \\ \omega\tilde{v} \end{bmatrix} \tag{2.10}$$

where O is zero matrix, I is identity matrix, and

$$\hat{M} = -\left[(1-v_0^2)\frac{\partial^2}{\partial z^2} - \left(3v_0 + \frac{1}{v_0}\right)\frac{\partial v_0}{\partial z}\frac{\partial}{\partial z} - \left(1 - \frac{1}{v_0^2}\right)\left(\frac{\partial v_0}{\partial z}\right)^2 - \left(v_0 + \frac{1}{v_0}\right)\frac{\partial^2 v_0}{\partial z^2}\right]$$

$$\hat{N} = -2i\left(v_0\frac{\partial}{\partial z} + \frac{\partial v_0}{\partial z}\right)$$

This becomes an algebraic eigenvalue problem if we discretize the operators and the function $\tilde{v}$.

2.6 Discretization

2.6.1 Finite Difference

Using these differentiation matrices, Eq.(2.10) becomes

$$\begin{bmatrix} O & I \\ M & N \end{bmatrix}\begin{bmatrix} \tilde{\mathbf{v}} \\ \omega\tilde{\mathbf{v}} \end{bmatrix} = \omega\begin{bmatrix} \tilde{\mathbf{v}} \\ \omega\tilde{\mathbf{v}} \end{bmatrix} \tag{2.11}$$

where O is a zero matrix, I is an identity matrix, and

$$M = -\text{diag}(1-\mathbf{v}_0^2)D^2 + \text{diag}\left(3\mathbf{v}_0 + \frac{1}{\mathbf{v}_0}\right)(D\mathbf{v}_0)D + \text{diag}\left(1 - \frac{1}{\mathbf{v}_0^2}\right)(D\mathbf{v}_0)^2 + \text{diag}\left(\mathbf{v}_0 + \frac{1}{\mathbf{v}_0}\right)(D^2\mathbf{v}_0)$$

$$N = -2i\left(\text{diag}(\mathbf{v}_0)D + D\mathbf{v}_0\right)$$

Here we abused the notation for the purpose of convenience, $\mathbf{v}_0^2$ means squaring every component of $\mathbf{v}_0$, and $1/\mathbf{v}_0$ denotes 1 divided by all components of $\mathbf{v}_0$.

Boundary Condition

We impose Dirichlet boundary condition on the problem, meaning that $\tilde{v}(-1) = \tilde{v}(1) = 0$. Further more, the differentiation matrices do not do well on the edges, so during the computation, we remove the first and last row of the differentiation matrices and the vectors $\tilde{\mathbf{v}}$ and $\mathbf{v}_0$. After the computation, we set $\tilde{v}_1 = \tilde{v}_N = 0$.

2.6.2 Spectral Element

Suppose the basis functions are $\{u_k(z)\}_{k=1}^{\infty}$, then the eigenfunction $\tilde{v}$ can be approximated by finite amount of them, $\tilde{v}(z) = \sum_{k=1}^{N} c_k u_k(z)$ where c_k are coefficients to be determined.

$$\begin{bmatrix} O & I \\ M & N \end{bmatrix} \begin{bmatrix} \mathbf{c} \\ \omega\mathbf{c} \end{bmatrix} = \omega \begin{bmatrix} \mathbf{c} \\ \omega\mathbf{c} \end{bmatrix} \tag{2.12}$$

where O is a zero matrix, I is an identity matrix, and

$$M_{jk} = -\int_{-1}^{1} dz\, u_j \left[(1-v_0^2)\frac{\partial^2}{\partial z^2} - \left(3v_0 + \frac{1}{v_0}\right)\frac{\partial v_0}{\partial z}\frac{\partial}{\partial z} - \left(1 - \frac{1}{v_0^2}\right)\left(\frac{\partial v_0}{\partial z}\right)^2 - \left(v_0 + \frac{1}{v_0}\right)\frac{\partial^2 v_0}{\partial z^2} \right] u_k$$

$$N_{jk} = -2i\int_{-1}^{1} dz\, u_j \left(v_0\frac{\partial}{\partial z} + \frac{\partial v_0}{\partial z}\right) u_k$$

Boundary Conditions and Basis Function

To satisfy the Dirichlet boundary condition, $\tilde{v}(\pm 1) = 0$, we can choose a set of basis functions that satisfy the boundary condition $u_k(\pm 1) = 0, \forall k \in \mathbb{N}$. For example, the sine functions

$$u_n(z) = \sin\Big(\frac{n\pi}{2}(z+1)\Big), n \in \mathbb{N}$$

is a set of basis functions that satisfy the Dirichlet boundary condition.

2.6.3 Finite Element

Finite-element method is a generalization of the spectral element method. We are allow to use a set of basis functions similar to spectral method in a cell. The region consists of many of these cells.

The formulation is the same as Eq.(2.12). The only difference is that in finite-element we need to solve Eq.(2.12) simultaneously for all cells.

Boundary Conditions and B-Spline

The B-Spline is a commonly used basis function for finite-element method. B-Spline can be defined recursively starting with piecewise constants [reference needed]

$$B_{i,0}(\xi) = \begin{cases} 1, & \text{if } \xi_i \leq \xi \leq \xi_{i+1} \\ 0, & \text{otherwise} \end{cases} \tag{2.13}$$

For $j \in \mathbb{N}$, they are defined by

$$B_{i,j}(\xi) = \frac{\xi - \xi_i}{\xi_{i+j} - \xi_i} B_{i,j-1}(\xi) + \frac{\xi_{i+j+1} - \xi}{\xi_{i+j+1} - \xi_{i+1}} B_{i+1,p-1}(\xi) \tag{2.14}$$

where $\xi = [\xi_0, \cdots, \xi_m]$ is called the knot vector, where $m = n + j + 1$ where $n + 1$ is the number of B-Splines and j is the degree of B-Spline polynomials. The knot vector defines the shapes of the B-Splines, see Fig.2.4. The variable ξ is within the range $[\xi_0, \xi_m]$.

Any function $u(x)$ on $[\xi_0, \xi_N]$ can be approximated by

$$u(x) \simeq \sum_{j=0}^{n} c_j B_{i,j}(x)$$

The Dirichlet boundary condition can be set by letting the coefficients of the first and last B-Spline to 0, $c_0 = c_n = 0$, where N is the number of B-Splines.

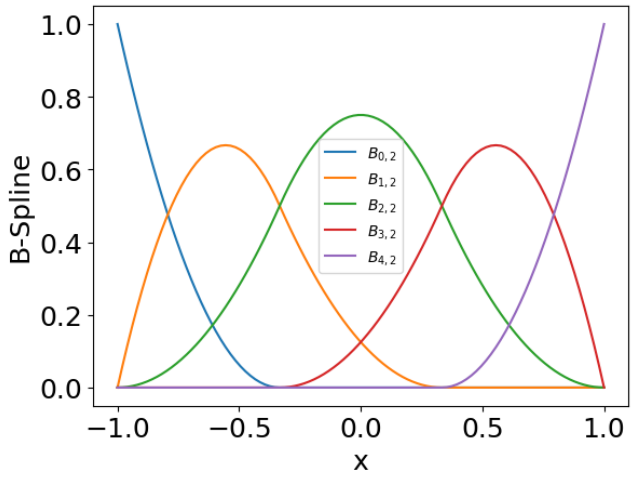

Figure 2.4: An example of open uniform quadratic B-Spline on $[-1, 1]$. The knot vector is $[-1, -1, -1, -1/3, 1/3, 1, 1, 1]$.

Chapter 3

Methodology

3.1 Spectral Method

3.1.1 Solve as Matrix Eigenvalue Problem

3.1.2 Discretization of Operators

3.1.3 Spectral Pollution

3.2 Shooting Method

3.2.1 Solve as Root Finding Problem

3.2.2 Expansion at Singularity

Chapter 4

Numerical Experiments

In this chapter, we will solve the eigenvalue problem, Eq.(2.10), with different discretizations. There will be three major categories of methods used. Finite difference (FD) method, finite element (FE) method and spectral element method (SE).

The finite difference method will be used together with equally spaced nodes. The finite element method will use B-spline as basis functions. Finally, the spectral element method uses sine functions as the spectral elements.

For Dirichlet boundary, The parameters of different discretizations are listed below

Table 4.1: With Dirichlet boundary condition, all methods have good accuracy, so using 101 nodes in the region $[0, 1]$ is enough. For FE and SE methods, they are using 50 basis functions.

	FD	FE_BSPLINE	SE_SINE
N	101	101	101
NUM_BASIS		51	50

For left-fixed and right-open (fixed-open) boundary condition, the parameters are

Table 4.2: With fixed-open boundary condition, it requires higher resolution in order to get accurate results. Therefore all methods use 501 nodes in the region $[0, 1]$, and FE method uses 101 basis functions.

	FD	FE_BSPLINE
N	501	501
NUM_BASIS		101

4.1 Constant Velocity Case

4.1.1 Dirichlet Boundary

Because the existence of exact solution to problems Eq.(**??**). The case with constant velocity profile is used as a sanity check. It allows us to verify the correctness of each method's implementation. This also serves as a reference to the accuracy spectral methods can achieve.

From Fig.(**??**), we see that the order of growth rates obtained by different methods is about 10^{-14} for both subsonic and supersonic cases. We will use these numbers as a reference to the accuracy of our numerical methods. If a method produces growth rates with order close to 10^{-14}, we consider the growth rates to be 0.

Table 4.3: Relative error of each eigenvalue.

$v_0 = 0.5$	1	2	3	4	5
FD	2.827e-05	1.130e-04	2.541e-04	4.512e-04	7.040e-04
FE	0.005	0.005	0.006	0.008	0.010
SE	2.896e-05	1.157e-04	2.603e-04	4.626e-04	7.217e-04

$v_0 = 1.5$	1	2	3	4	5
FD	0.001	0.005	0.010	0.019	0.030
FE	0.006	0.010	0.019	0.029	0.043
SE	0.001	0.005	0.011	0.019	0.030

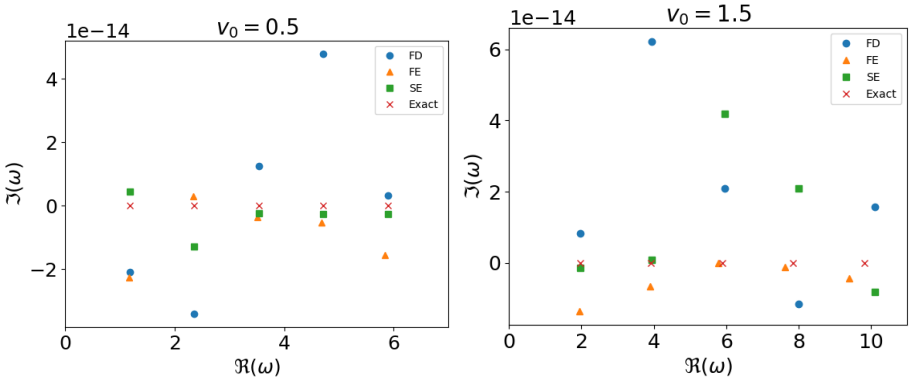

(a) All modes are stable.

(b) Filtered modes are stable.

Figure 4.1: Showing the first 5 eigenvalues of each method in each case. All methods are close to the exact eigenvalues.

4.1.2 Fixed-Open Boundary

Table 4.4: Relative error of each eigenvalue. Notice that the ground mode for subsonic case is non-zero.

$v_0 = 0.5$	0	1	2	3	4
FD	1.209e-05	3.458e-05	5.775e-05	8.153e-05	1.061e-04
FE	8.090e-05	2.007e-04	2.981e-04	6.596e-04	1.821e-03
$v_0 = 1.5$	1	2	3	4	5
FD	9.163e-05	2.435e-04	4.833e-04	8.160e-04	1.243e-03
FE	4.431e-04	7.924e-04	1.516e-03	3.103e-03	8.001e-03

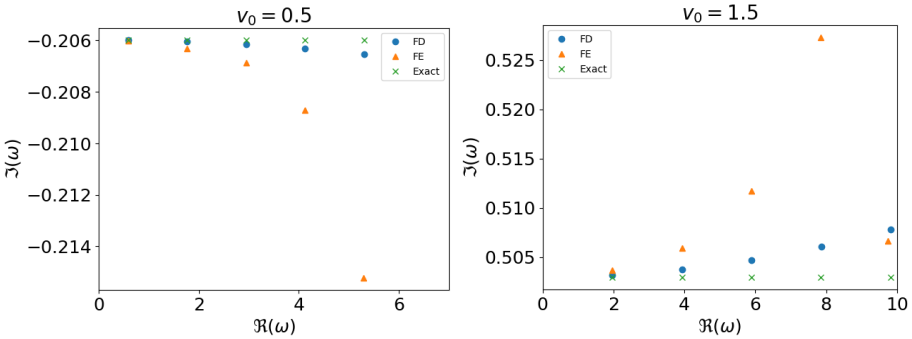

(a) All modes are stable.

(b) All modes are unstable.

Figure 4.2: Showing the first 5 eigenvalues of each method. Finite-difference method has much better accuracy than finite-element method.

4.2 Subsonic Case

4.2.1 Dirichlet Boundary

When setting the mid-point velocity to be $M_m = 0.5$, we have the subsonic velocity profile. This velocity profile is the orange line shown in Fig.2.3. With Dirichlet boundary condition, $\tilde{v}(\pm 1) = 0$. The flow in magnetic nozzle is stable. Fig.4.3 shows the first few eigenvalues obtained by different discretizations.

The order of growth rates obtained by different methods is 10^{-13}, we can consider it to be stable.

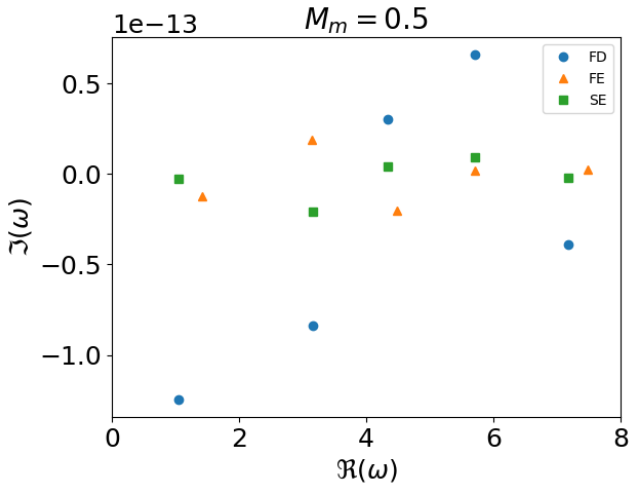

Figure 4.3: Showing the first 5 modes. It suggests that the flow in magnetic nozzle with subsonic velocity profile and Dirichlet boundary condition is stable.

4.2.2 Fixed-Open Boundary

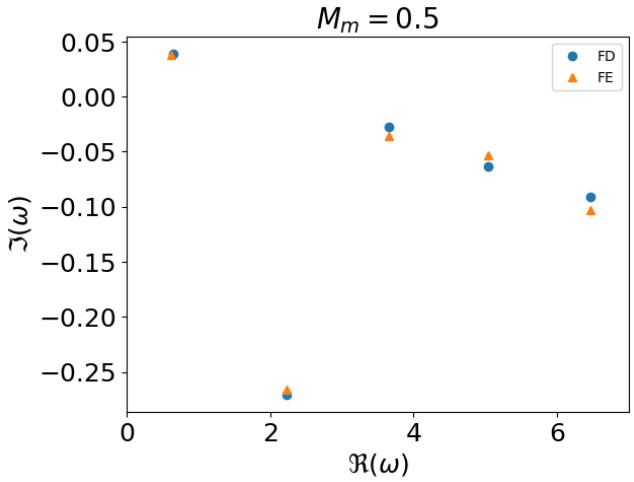

Figure 4.4: Showing the first 5 modes. The ground mode is unstable, other modes are stable.

4.3 Supersonic Case

4.3.1 Dirichlet Boundary

When the velocity profile is supersonic, shown as purple line in Fig.2.3, spurious modes appeared as predicted in Chap.**??**. Using the convergence test, we successfully eliminates all unstable modes. Fig.(4.5) shows the first few filtered eigenvalues. As we can see the flow is stable.

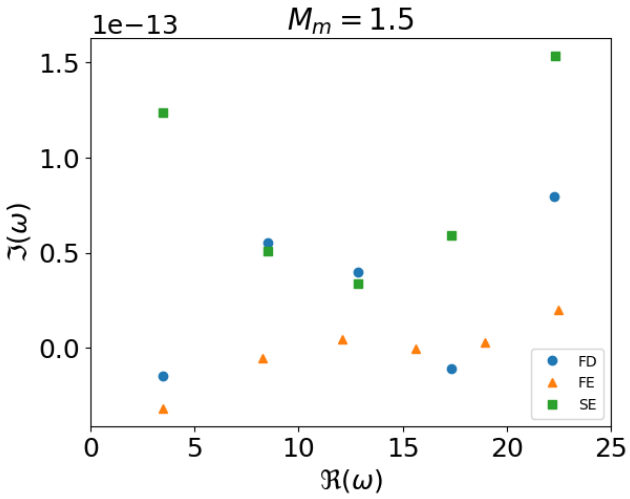

Figure 4.5: First few filtered eigenvalues are shown. The spurious modes are filtered by convergence test.

4.3.2 Fixed-Open Boundary

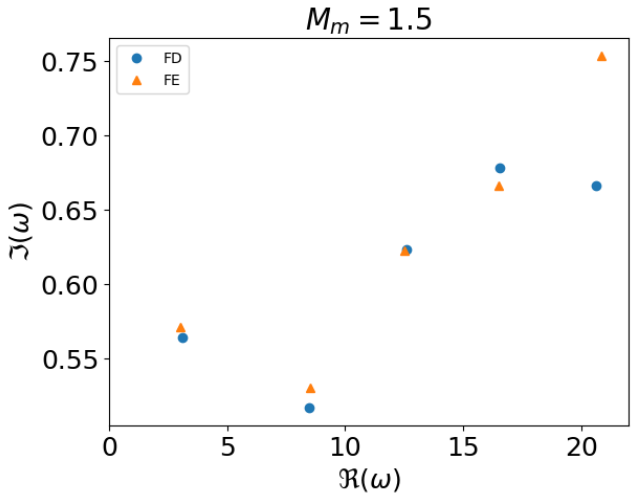

Figure 4.6: All modes are unstable.

4.4 Accelerating Case

Starting from the singular point, we shoot the solution to the left boundary. We find the set of eigenvalues such that $\tilde{v}(-1) = 0$. With these eigenvalues, we can extend the solution to the supersonic region $(0, 1]$. The first five eigenvalues are drawn in the graph.

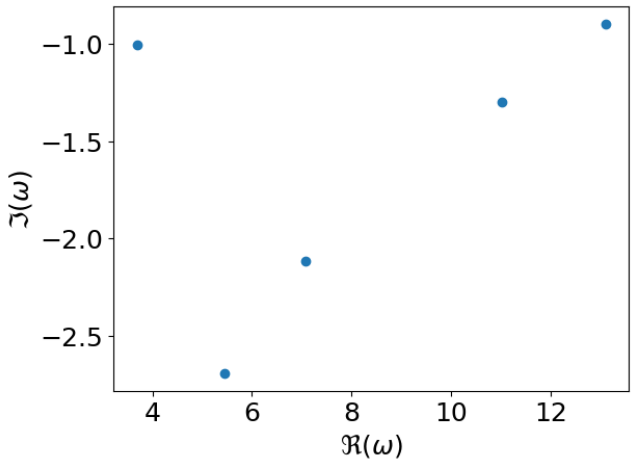

Figure 4.7: first five modes are stable.

Chapter 5

conclusion

In chapter 3, we derived the linearized equations of motion of the flow in one dimensional magnetic nozzle. Furthermore, we rewrite the linearized governing equations as an eigenvalue problem. Using the spectral methods introduced in chapter 2, we discretized the operators of the problem. Hence transforming it into an algebraic eigenvalue problem.

With the aid of computer, we are able to solve the algebraic eigenvalue problem. The results show that the flow in magnetic nozzle with Dirichlet boundary condition is stable except the case with decelerating velocity profile.

Bibliography

[1] Toshiki Aikawa. The stability of spherically symmetric accretion flows. *Astrophys Space Sci*, 66(2):277–285, December 1979.